26. Winfield, D. A. The postnatal development of synapses in the visual cortex of the cat and the effects of eyelid closure. *Brain Res.* **206,** 166–171 (1981).
27. Vees, A. M., Micheva, K. D., Beaulieu, C. & Descarries, L. Increased number and size of dendritic spines in ipsilateral barrel field cortex following unilateral whisker trimming in postnatal rat. *J. Comp. Neurol.* **400,** 110–124 (1998).
28. Movshon, J. A. & Dursteler, M. R. Effects of brief periods of unilateral eye closure on the kitten's visual system. *J. Neurophysiol.* **40,** 1255–1265 (1977).
29. Simons, D. J. & Land, P. W. Early experience of tactile stimulation influences organization of somatic sensory cortex. *Nature* **326,** 694–697 (1987).
30. Schlaggar, B. L., Fox, K. & O'Leary, D. D. M. Postsynaptic control of plasticity in developing somatosensory cortex. *Nature* **364,** 623–626 (1993).

Acknowledgements

We thank B. Burbach and E. Nimchinsky for help with experiments, K. Greenwood for help with analysis, Z. Mainen, M. Maravall, E. Ruthazer and B. Sabatini for comments on the manuscript, and the Malinow laboratory for help with viruses. This work was supported by IBRO (BL), HFSP, the Mathers and Pew Foundations (K.S.) and an NIH training grant to SHNY Stony Brook (B.C.).

Correspondence and requests for materials should be addressed to K.S. (e-mail: svoboda@cshl.org).

Ion permeation mechanism of the potassium channel

Johan Åqvist* & Victor Luzhkov*†

* *Department of Cell and Molecular Biology, Uppsala University, Biomedical Center, Box 596, SE-751 24 Uppsala, Sweden*

Ion-selective channels enable the specific permeation of ions through cell membranes and provide the basis of several important biological functions; for example, electric signalling in the nervous system[1]. Although a large amount of electrophysiological data is available[1,2], the molecular mechanisms by which these channels can mediate ion transport remain a significant unsolved problem. With the recently determined crystal structure of the representative K^+ channel (KcsA) from *Streptomyces lividans*[3], it becomes possible to examine ion conduction pathways on a microscopic level. K^+ channels utilize multi-ion conduction mechanisms[1,2,4–6], and the three-dimensional structure also shows several ions present in the channel. Here we report results from molecular dynamics free energy perturbation calculations that both establish the nature of the multiple ion conduction mechanism and yield the correct ion selectivity of the channel. By evaluating the energetics of all relevant occupancy states of the selectivity filter, we find that the favoured conduction pathway involves transitions only between two main states with a free difference of about 5 kcal mol^{-1}. Other putative permeation pathways can be excluded because they would involve states that are too high in energy.

The KcsA channel is a membrane-spanning tetrameric assembly with a narrow selectivity filter for permeating ions near its extracellular side, as well as a relatively large water-filled cavity near the centre of the membrane[3] (Fig. 1). These two structural features provide a stabilizing environment for ions passing through the channel that allows them to surpass the high energy barrier otherwise imposed by the nonpolar membrane interior. The filter region, which corresponds to the highly conserved signature sequence (TVGYG), comprises four more-or-less distinct binding sites that are occupied by ions or water molecules. These sites are separated by 3.4 Å, 3.9 Å and 3.3 Å in the crystal structure (Protein Data Bank (PDB) entry 1bl8)[3] which sterically allows their simultaneous occupation by four particles (K^+ ions or water molecules, both with a typical radius of 1.4 Å). This four-site structure gives rise to 16 theoretically possible loading states of the filter (Fig. 2). The main problem in determining the ion conduction mechanism is thus to find the energetically most favourable pathway that connects a subset of these states in a cyclic fashion, resulting in a net translocation of ions across the membrane. It may be seen from the combinatorial scheme that there are several possible permeation cycles of varying complexity, involving different number of loading states. We consider here the inward flux direction as observed in typical patch-clamp experiments under hyperpolarized conditions[7]. Figure 2 depicts only the pathways that result from 'single-file' movement through the selectivity filter; that is, ions/waters occupying the four filter positions will then all be shifted inwards one step as an ion or water molecule moves into the first position, and the species occupying the fourth position is released into the cavity region.

Experimental current–voltage relationships for typical K^+ channels (including KcsA), as well as gramicidin, yield conductance values in the tens of picosiemens range[2,7,8]. When these results are interpreted in terms of kinetic barrier models for ion permeation, activation free energies of around 5–7 kcal mol^{-1} are predicted[1,2,8–12]. Although the qualities of different models for ion permeation are still under debate[12,13], this type of estimate does establish an upper limit for the energy barriers involved in the process. To find the operational translocation mechanism for K^+ ions, we calculated the relative free energies of different configurations in Fig. 2 with the molecular dynamics (MD) free energy perturbation (FEP) technique[14–16]. This involves the evaluation of free energies of binding ions from an external solution, as well as of permuting ion and water positions inside the filter. In all simulations the channel tetramer

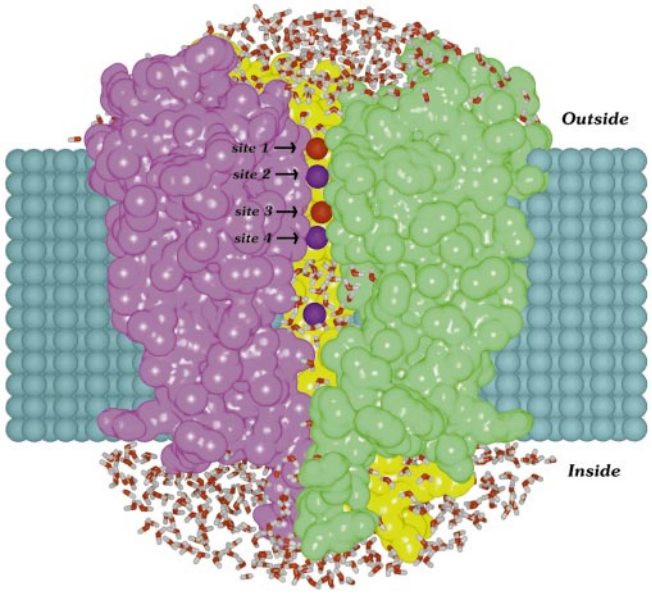

Figure 1 View of the solvated KcsA channel in which one of the four subunits has been omitted from the picture to make the pore visible. The filter region near the extracellular side is ~12 Å long with backbone carbonyl groups facing the pore, thereby providing stabilization of ions through interaction with their dipoles. The central cavity below the filter can accommodate a number of water molecules (around 30), and the diffuse electron density observed experimentally in this region shows the presence of a solvated ion[3]. The depicted structure has two water molecules (red spheres) and two ions (blue) in the selectivity filter and one in the central water-filled cavity. The channel is embedded in a cylindrical model membrane in all calculations.

† Permanent address: Institute of Chemical Physics Problems, Russian Academy of Sciences, Chernogolovka, Moscow Region 142432, Russian Federation.

was embedded in a model membrane and solvated by a large sphere of water molecules, which covers the channel openings and also fills up the internal cavity with solvent (Fig. 1). The conclusions presented here are the result of extensive MD/FEP calculations, in which the sensitivity to initial conditions and simulation set-up has been carefully gauged (see Methods).

The K^+ channel turns out to have a preference for accommodating altogether three ions, two in the selectivity filter and one in the central water-filled cavity. The most stable configuration of the filter is found to be that with the second and fourth positions (counting from the extracellular side) occupied by ions, and the first and third positions by water molecules. We will refer to the different occupancy states by a binary code, so that the most stable state is denoted 0101(1) where the last '(1)' simply states that the cavity ion is also present. In fact, 'binding' of the cavity ion is calculated to be favourable for all two-ion states (referring to the occupancy of the filter) by 1–5 kcal mol^{-1}. The finding that the lowest free energy is obtained with two ions in the filter and one in the cavity is completely in accord with experimental results[1–6]. Recent dielectric continuum calculations[17] also showed stabilization of the cavity ion by several kilocalories per mole. The most stable single-occupancy state of the filter, namely 0100(1), has a free energy of 2.4 kcal mol^{-1} above 0101(1); however, the other configurations with one ion in the filter lie 10–15 kcal mol^{-1} above 0101(1). This implies that a translocation mechanism with only one ion at a time moving through the selectivity filter is energetically unfavourable, as the corresponding activation energy would be at least 15 kcal mol^{-1} with a very low resulting conductance. There are still a number of possible mechanisms that do not involve any of the high-energy singly occupied configurations (compare Fig. 2); however, our calculations also show that the states with three ions in the filter are all higher in energy than the resting state 0101(1). Among these three-ion states only 1101(1) has a non-prohibitive free energy relative to the resting state, which, in effect, excludes any mechanism involving the three-ion states.

The energetic summary in Fig. 2 shows that the most favourable pathway for ion translocation through the filter is the simple cycling between states 1010(1) and 0101(1), where the latter configuration also was found to be the resting state of the channel. The free energy difference between 1010(1) and 0101(1) is only about 5 kcal mol^{-1}, whereas the other possible two-ion mechanism 1100⟶ 0110⟶ 0011 ⟶ 1001⟶ 1100… is associated with free energy barriers well over 10 kcal mol^{-1} relative to the resting state. Although collective single-file movement is usually considered to be the case in channel conduction, it is also possible that exchange could take place at the first and fourth filter position without any file movement. However, because the singly and triply occupied states are in essence energetically prohibited, ion/water exchange would have no influence on the mechanistic conclusions. In our calculations, we have considered the case with no net free energy change associated with ion translocation across the membrane, which refers to the absence of an electrochemical driving force for ionic current through the channel (similar to the equilibrium polarized state of the cell membrane).

Although the 1010(1)↔0101(1) mechanism remains the only alternative that is thermodynamically compatible with a high flux of ions through the channel, there could, in principle, be high activation barriers associated with passage between the two states. Calculation of the entire free energy profile, or potential of mean force, for translocation of ions across the membrane would be difficult owing to the presumably coupled movement of ions/waters inside the filter and near its openings. This is particularly relevant to the loading and release of ions from the selectivity filter, as calculation of statistically meaningful paths for ion movement in the solvent near the filter presents a conceptually hard problem. But for the restricted part of this process corresponding to the single-file movement from 1010(1) to 0101(1), including water entering and leaving the filter, the calculation is straightforward to do, by just considering local displacements within the filter. Figure 3 shows the resulting free energy profile; it may be seen that, in agreement with the thermodynamic perturbation results above, the 0101(1) state is a rather wide and stable minimum on the free energy surface. The configuration 1010(1), on the other hand, corresponds to a high-energy region. The estimated activation barrier for passage from 1010(1) to 0101(1) is around 6 kcal mol^{-1}, and the free energy profile is also in reasonable agreement with the independent FEP results for the free energy difference between these states. Although the calculation in Fig. 3 only provides part of the reaction profile for the two-state translocation mechanism, it is still informative in that it shows that the higher energy state is energetically close to the barrier along this part of the profile. The release of ions from the interior cavity to the intracellular side will presumably be coupled to the cycling of ions through the channel filter. This latter process is not likely to be associated with large energy barriers as there is no narrow filter that must be surpassed and because the calculated solvation energies of ions in the cavity are close to those in bulk solution.

An essential feature of ion-selective channels is their ability to discriminate between different ion species; K^+ channels are known to have a conductivity for Na^+ that is several orders of magnitude lower than for K^+, whereas Rb^+ permeation rates are usually comparable to those for K^+ (refs 1, 2). To examine the selectivity of KcsA, we performed FEP calculations on the 0101(1) (low

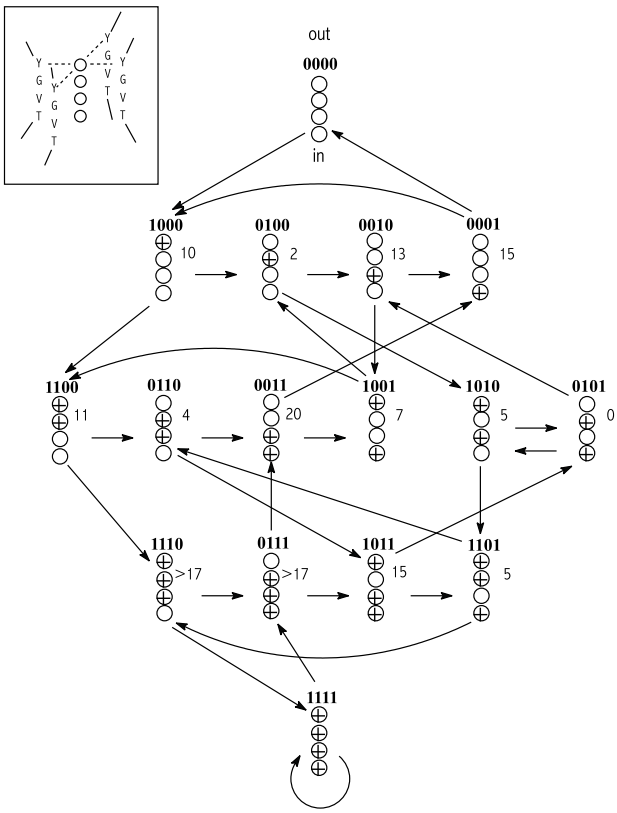

Figure 2 The different possible loading states of the four-site selectivity filter. A given site is occupied either by an ion (circle with a cross) or a water molecule (circle). The arrows denote ion translocation pathways resulting from single-file movement inwards when an additional ion or water molecular enters the filter from the outside. This directionality of permeation corresponds to an inward current[7]. The calculated energetics is given (in kcal mol^{-1}) relative to the most stable state, and all free energies refer to the case with the experimentally observed cavity ion present. The insets show schematically the position of ion-binding sites within the (tetrameric) signature motif.

energy) and 1010(1) (high energy/barrier) configurations, where the two ions in the filter were simultaneously mutated from K^+ to Na^+ and Rb^+, respectively. Among other effects, this approach accounts for the essential role of protein relaxation in selectivity. The results show that both of these states are selective for K^+, with relative binding free energies of $\Delta\Delta G_{bind}(K^+ \rightarrow Na^+) = +4.5$ kcal mol^{-1} and $\Delta\Delta G_{bind}(K^+ \rightarrow Rb^+) = +2.6$ kcal mol^{-1} for state 1010, and $\Delta\Delta G_{bind}(K^+ \rightarrow Na^+) = +1.0$ kcal mol^{-1} and $\Delta\Delta G_{bind}(K^+ \rightarrow Rb^+) = +0.9$ kcal mol^{-1} for state 0101. A reasonable estimate for the difference in activation free energy should thus be provided by subtracting the relative binding energies in the low-energy state from those in the high-energy state. This yields $\Delta\Delta G^{\ddagger}(K^+ \rightarrow Na^+) = +3.5$ kcal mol^{-1} and $\Delta\Delta G^{\ddagger}(K^+ \rightarrow Rb^+) = +1.7$ kcal mol^{-1} (the typical error bars for these calculations are $\pm$ 0.5 kcal mol^{-1}). Therefore, the calculations predict, in terms of transition-state theory, a permeability ratio for K^+ over Na^+ of 100–1,000 whereas that over Rb^+ is only around 20. These predictions appear to agree well with typical experimental values for K^+ channels[2], although selectivity measurements often involve mixed ionic solutions. Furthermore, the result that the high-energy state is more strongly selective for K^+ over Na^+ than the resting state is very reasonable. That is, the configuration corresponding to the barrier or transition-state region should be most discriminatory against such ions, while the low-energy state should be less sensitive[10].

With regard to structural factors controlling the energetics of the selectivity filter, it appears that the two interior filter sites (sites two and three) have a key role as they are not in direct contact with bulk solvent on either side of the filter. Here, it is clear that site two provides the strongest ion stabilization of all sites, while the third site is considerably less favourable. The reason for this is both that the cavity formed by the carbonyl groups is smaller at the second site and that the orientations of the eight surrounding carbonyls are more favourable. Single-ion perturbation calculations in the state 1010(1) also show that it is at the third position where the main part of the selectivity against Na^+ is exerted. However, other factors—such as the ion–ion repulsion and water–protein interactions inside the filter, as well as the helix dipoles directed towards the interior cavity—contribute to the subtle energetic balance of the structure. Unfortunately, the crystal structure of the *Streptomyces lividans* channel at 3.2 Å resolution[3] does not provide conclusive information regarding the stable positions of K^+ ions in the channel in its physiological environment. However, the difference maps with Rb^+ and Cs^+ were interpreted in terms of two ions separated by about 7.5 Å occupying the filter. Such a configuration would presumably be compatible with either of the two states involved in our mechanism. On the other hand, it is important to realize that the crystal structure corresponds to a head-to-head packing of channels in which the extracellular faces are stacked onto each other[3], and that the protein tetramers are surrounded by a polar solution rather than a low-dielectric membrane medium. These types of differences in the local environment around the protein, compared with the physiological situation, may well shift the fine energy balance enough for any of the lowest lying occupancy states to be observed.

The main principles of ion stabilization in the KcsA K^+ channel selectivity filter are similar to those in several other systems (for example, the gramicidin A channel, certain ionophores and ion-binding sites in icosahedral viruses), although the architecture of the selectivity filter gives rise to considerable mechanistic complexity. We have shown how a number of different ion permeation mechanisms can result from such a structure (Fig. 2). However, when evaluating the energetics of all relevant loading states of the channel, one such mechanism emerges as the most likely candidate. □

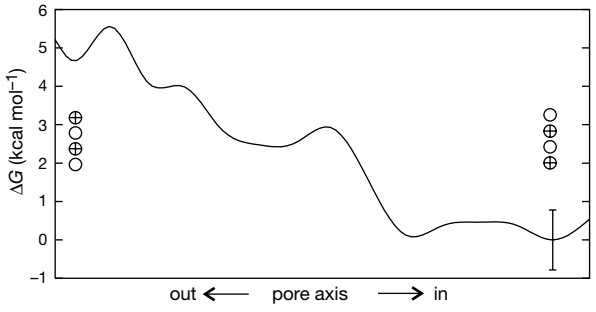

Figure 3 Free energy profile (potential of mean force) for the single-file movement between the 1010(1) and 0101(1) states. The profile was calculated by successive restraining of the two filter ions to 50 different planes along the pore axis, spanning the 3–4 Å spatial range between the two configurations. During this process one water molecule is pushed out of the selectivity filter into the cavity and a new water molecule spontaneously enters the filter from the outside, as might be expected.

Methods

The molecular model used in all simulations consists of the channel tetramer embedded in a cylindrical slab of hydrocarbon-like atoms representing the membrane and solvated by a sphere of water; the latter has a radius of about 33 Å, and is centred near the middle of the selectivity filter (Fig. 1). The crystallographic structure of the KcsA channel (PDB entry 1bl8)[3], both with and without the missing sidechains (Arg 27, Ile 60, Arg 64, Glu 71 and Arg 177) built in, was used as the starting point for MD calculations. The sensitivity of the computational model, both to the inclusion of these sidechains and to the size of the membrane slab and water sphere, was carefully checked, and very similar results were obtained with a number of different set-ups (for example, the thickness of the membrane slab was varied between 30 Å and 34 Å, and water spheres with radii between 25 Å and 34 Å were examined). Four different types of free energy calculation schemes were used. (1) For binding of an additional K^+ to a given loading state (that is, moving downwards in Fig. 2), the forward and reverse free energy of transformation between an ion and a water molecule at the given site was calculated and compared with the corresponding result in a 33 Å sphere of pure water. (2) For calculating relative energies between states with the same overall ion occupancy (that is, moving horizontally in Fig. 2), multiple transformations of this kind were carried out simultaneously in the channel. (3) Selectivity calculations were done in the standard way by transformation between different ion species inside the channel filter and in water. In all of the above types of simulations, ions and waters in the filter were restrained to planes perpendicular to the channel axis to ensure the integrity of different loading states. In the selectivity calculations, only one (ion) position was restrained to allow relaxation along the axis. Most calculations were repeated with several different harmonic force constants for the restraints (0.5, 3.0, 5.0, 10.0 and 100.0 kcal mol^{-1} Å^{-2}) and no severe dependencies on these were found. (4) The free energy profile for motion between states 1010(1) and 0101(1) was carried out in a standard manner by successive restraining of the two filter ions to different planes along the pore axis[11]. In the binding calculations, the system was made overall neutral before insertion of the additional ion to avoid the dielectric artefacts of using a finite system[18]. Both binding and selectivity calculations were repeated with several different distributions of net charges on ionizable groups to examine possible dependencies on such choices. Furthermore, the network connecting the different states (Fig. 2) allows for a critical estimation of errors by evaluating the closure of many thermodynamic cycles in the network. The error range emerging from the considerations above is typically $\leq$1 kcal mol^{-1} for the low energy states of Fig. 2, and $\leq$2–3 kcal mol^{-1} for the high-energy states.

All MD calculations were performed with the program Q (ref. 19) using the Gromos87 force field[20] together with ion parameters that reproduce experimental solvation energies[21]. Protein–protein, protein–water and water–water long-range electrostatics were treated with a third-order multipole expansion method[22], whereas all interactions involving the ions were explicitly calculated. Water bonds and angles, as well as all protein bondlengths, were constrained using the SHAKE procedure[23]. The simulations were carried out at 300 K using an MD time step of 2 fs. Each FEP transformation involved 50–70 ps of equilibration followed by 100 ps of data sampling, where 50 different values of the FEP coupling parameter[14–16] were used. Each such transformation was run independently in both the forward and reverse direction. The energetics in Fig. 2 are the result of evaluating 60–70 different transformation legs between loading states, and each such calculation was repeated for several set-ups as discussed above.

Received 8 September 1999; accepted 10 February 2000.

1. Hille, B. *Ionic Channels of Excitable Membranes* (Sinauer, Sunderland, Massachusetts, 1992).
2. Latorre, R. & Miller, C. Conduction and selectivity in potassium channels. *J. Membr. Biol.* **71,** 11–30 (1983).
3. Doyle, D. A. *et al.* The structure of the potassium channel: molecular basis of K^+ conduction and selectivity. *Science* **280,** 69–77 (1998).
4. Hodgkin, A. L. & Keynes, R. D. The potassium permeability of a giant nerve fibre. *J. Physiol.* **128,** 61–88 (1955).
5. Hille, B. & Schwarz, W. Potassium channels as multi-ion single-file pores. *J. Gen. Physiol.* **72,** 409–442 (1978).
6. Begenisich, T. & de Weer, P. Potassium flux ratio in voltage-clamped squid giant axons. *J. Gen. Physiol.* **76,** 83–98 (1980).

7. Schrempf, H. *et al.* A prokaryotic potassium ion channel with two predicted transmembrane segments from *Streptomyces lividans*. *EMBO J.* **14,** 5170–5178 (1995).
8. Bamberg, E. & Läuger, P. Temperature-dependent properties of gramicidin A channels. *Biochim. Biophys. Acta* **367,** 127–133 (1974).
9. Hladky, S. B. & Haydon, D. A. Ion transfer across lipid membranes in the presence of gramicidin A. *Biochim. Biophys. Acta* **274,** 294–312 (1972).
10. Eisenman, G. & Horn, R. Ion selectivity revisited: the role of kinetic and equilibrium processes in ion permeation through channels. *J. Membr. Biol.* **76,** 197–225 (1983).
11. Roux, B. & Karplus, M. Ion transport in a gramicidin-like channel: dynamics and mobility. *J. Phys. Chem.* **95,** 4856–4868 (1991).
12. McCleskey, E. W. Calcium channel permeation: a field in flux. *J. Gen. Physiol.* **113,** 765–772.
13. Miller, C. Ionic hopping defended. *J. Gen. Physiol.* **113,** 783–787 (1999).
14. van Gunsteren, W. F. & Berendsen, H. J. C. Computer simulation of molecular dynamics: methodology, applications and perspectives in chemistry. *Angew. Chem. Int. Edn Engl.* **29,** 992–1023 (1990).
15. Karplus, M. & Petsko, G. A. Molecular dynamics simulations in biology. *Nature* **347,** 631–639 (1990).
16. Kollman, P. Free energy calculations: applications to chemical and biochemical phenomena. *Chem. Rev.* **93,** 2395–2417 (1993).
17. Roux, B. & MacKinnon, R. The cavity and pore helices in the KcsA K^+ channel: electrostatic stabilization of monovalent cations. *Science* **285,** 100–102 (1999).
18. Åqvist, J. Calculation of absolute binding free energies for charged ligands and effects of long-range electrostatic interactions. *J. Comput. Chem.* **17,** 1587–1597 (1996).
19. Marelius, J., Kolmodin, K., Feierberg, I. & Åqvist, J. Q: a molecular dynamics program for free energy calculations and empirical valence bond simulations in biomolecular systems. *J. Mol. Graph. Model.* **16,** 213–225 (1998).
20. van Gunsteren, W. F. & Berendsen, H. J. C. *Groningen Molecular Simulation (GROMOS) Library Manual* (Biomos B.V., Groningen, The Netherlands, 1987).
21. Åqvist, J. Ion-water interaction potential derived from free energy perturbation simulations. *J. Phys. Chem.* **94,** 8021–8024 (1990).
22. Lee, F. S. & Warshel, A. A local reaction field method for fast evaluation of long-range electrostatic interactions in molecular simulations. *J. Chem. Phys.* **97,** 3100–3107 (1992).
23. Ryckaert, J. P., Ciccotti, G. & Berendsen, H. J. C. Numerical integration of the Cartesian equations of motion of a system with constraints. *J. Comput. Phys.* **23,** 327–341 (1977).

Acknowledgements

We thank T. A. Jones for comments and M. R. Harris for graphics. This work was supported by the Wenner–Gren Foundation and the Swedish Natural Science Research Council (NFR).

Correspondence and requests for materials should be addressed to J.Å. (e-mail: aqvist@xray.bmc.uu.se).

CD1c-mediated T-cell recognition of isoprenoid glycolipids in *Mycobacterium tuberculosis* infection

D. Branch Moody*, Timo Ulrichs*†, Walter Mühlecker‡, David C. Young‡, Sudagar S. Gurcha§, Ethan Grant*, Jean-Pierre Rosat*, Michael B. Brenner*, Catherine E. Costello‡, Gurdyal S. Besra§ & Steven A. Porcelli*†

* *Division of Rheumatology, Immunology and Allergy, Brigham and Women's Hospital and Harvard Medical School, Boston, Massachusetts 02115, USA*
‡ *Mass Spectrometry Resource, Boston University School of Medicine, Boston, Massachusetts 02118, USA*
§ *Department of Microbiology and Immunology, The Medical School, University of Newcastle Upon Tyne, Framlington Place, Newcastle upon Tyne NE2 4HH, UK*

The discovery of the CD1 antigen presentation pathway has expanded the spectrum of T-cell antigens to include lipids[1–4], but the range of natural lipid antigens and functions of CD1-restricted T cells *in vivo* remain poorly understood. Here we show that the T-cell antigen receptor and the CD1c protein mediate recognition of an evolutionarily conserved family of isoprenoid glycolipids whose members include essential components of protein glycosylation and cell-wall synthesis pathways. A CD1c-restricted, mycobacteria-specific T-cell line recognized two previously unknown mycobacterial hexosyl-1-phosphoisoprenoids and structurally related mannosyl-β1-phosphodolichols. Responses to mannosyl-β1-phosphodolichols were common among CD1c-restricted T-cell lines and peripheral blood T lymphocytes of human subjects recently infected with *M. tuberculosis*, but were not seen in naive control subjects. These results define a new class of broadly distributed lipid antigens presented by the CD1 system during infection *in vivo* and suggest an immune mechanism for recognition of senescent or transformed cells that are known to have altered dolichol lipids.

CD1a, CD1b and CD1c, three members of the human CD1 family of major histocompatibility complex (MHC) class I-like cell-surface glycoproteins, present bacterial lipid antigens for recognition by T cells[4–8]. A small number of mycobacterial lipid antigens presented by CD1b have been purified to homogeneity and identified[4–6], and structural studies of these antigens and of the CD1 proteins have led to the proposal of a general molecular mechanism for lipid antigen presentation by CD1 (refs 9, 10). This involves the binding of the alkyl components of the antigens within a hydrophobic groove in

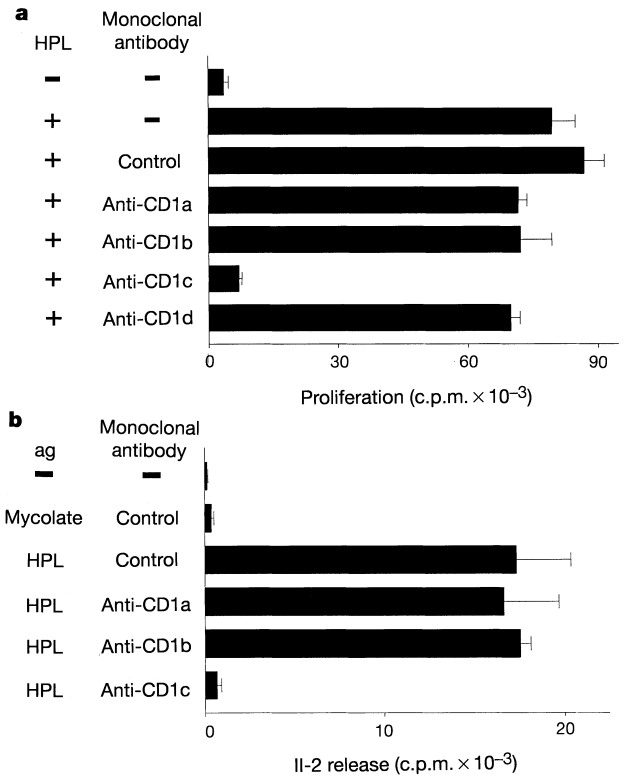

Figure 1 Molecular requirements for T-cell recognition of a hexosyl phospholipid (HPL) antigen. **a**, CD8-1 T cells and irradiated monocyte-derived dendritic cells were cultured for 3 d with the HPL antigen (0.5 μg ml^{-1}) and the monoclonal antibody specific for the indicated CD1 isoform (20 μg ml^{-1}); T-cell proliferation was determined by ^{3}H-thymidine incorporation[7,8]. **b**, The TCR α- and β-chains from T-cell line CD8-1 (TCRAV1S3J17C1, TCRBV2S1J2S7C2) were cloned into the pREP7 and pREP9 expression vectors and transfected into CD3$^-$ J.RT3 T lymphoblastoid cells[13]. J.RT3 transfectants were cultured with irradiated monocyte-derived dendritic cells, antigen (mycolate 50 μg ml^{-1}, HPL 0.5 μg ml^{-1}), blocking antibody (20 μg ml^{-1}) and phorbol myristate acetate (10 ng ml^{-1}; Sigma). Levels of IL-2 released were determined by measuring ^{3}H-thymidine incorporation by HT-2 cells[13]. JRT.3 cells similarly transfected with TCR α- and β-chains from the CD1b-restricted line LDN5 and the CD1a-restricted line CD8-2 did not respond to the *M. avium* HPL (data not shown)[6,7].

† Present Address: Department of Microbiology and Immunology, Albert Einstein College of Medicine, Room 416 Forchheimer Building, 1300 Morris Park Avenue, Bronx, New York 10461, USA.